Charged meson rapidity distributions in central Au+Au collisions at $\sqrt{s_{NN}} = 200\,\mathrm{GeV}$

I. G. Bearden[7], D. Beavis[1], C. Besliu[10], B. Budick[6], H. Bøggild[7], C. Chasman[1], C. H. Christensen[7], P. Christiansen[7], J. Cibor[3], R. Debbe[1], E. Enger[12], J. J. Gaardhøje[7], M. Germinario[7], K. Hagel[8], O. Hansen[7], A. Holm[7], A. K. Holme[12], H. Ito[11], A. Jipa[10], F. Jundt[2], J. I. Jørdre[9], C. E. Jørgensen[7], R. Karabowicz[4], E. J. Kim[11], T. Kozik[4], T. M. Larsen[12], J. H. Lee[1], Y. K. Lee[5], G. Løvhøiden[12], Z. Majka[4], A. Makeev[8], M. Mikelsen[12], M. Murray[11], J. Natowitz[8], B. S. Nielsen[7], J. Norris[11], K. Olchanski[1], D. Ouerdane[7], R. Płaneta[4], F. Rami[2], C. Ristea[10], D. Röhrich[9], B. H. Samset[12], D. Sandberg[7], S. J. Sanders[11], R. A. Sheetz[1], P. Staszel[7], T. S. Tveter[12], F. Videbæk[1], R. Wada[8], Z. Yin[9], and I. S. Zgura[10]
(BRAHMS Collaboration)

[1] Brookhaven National Laboratory, Upton,New York 11973,
[2] Institut de Recherches Subatomiques and Université Louis Pasteur, Strasbourg, France,
[3] Institute of Nuclear Physics, Krakow, Poland,
[4] Jagiellonian University, Krakow, Poland,
[5] Johns Hopkins University, Baltimore, Maryland 21218,
[6] New York University, New York, New York 10003,
[7] Niels Bohr Institute, University of Copenhagen, Denmark,
[8] Texas A&M University, College Station,Texas 77843,
[9] University of Bergen, Department of Physics, Bergen,Norway,
[10] University of Bucharest,Romania,
[11] University of Kansas, Lawrence, Kansas 66049,
[12] University of Oslo, Department of Physics, Oslo,Norway

We have measured rapidity densities dN/dy of $\pi^{\pm}$ and $K^{\pm}$ over a broad rapidity range ($-0.1 < y < 3.5$) for central Au+Au collisions at $\sqrt{s_{NN}} = 200\,\mathrm{GeV}$. These data have significant implications for the chemistry and dynamics of the dense system that is initially created in the collisions. The full phase–space yields are $1742 \pm 17 \pm 140$ (π^+), $1761 \pm 16 \pm 141$ (π^-), $288 \pm 5 \pm 23$ (K^+) and $241 \pm 3 \pm 19$ (K^-). The systematics of the strange to non–strange meson ratios are found to track the variation of the baryo–chemical potential with rapidity and energy. Landau–like hydrodynamic is found to describe the bulk transport of the pions in the longitudinal direction.

In ultra–relativistic heavy ion collisions at RHIC energies, charged pions and kaons are produced copiously. The yields of these light mesons are indicators of the entropy and strangeness created in the reactions, sensitive observables to the possible existence of an early color deconfined phase, the so–called quark gluon plasma. In such collisions, the large number of produced particles and their subsequent reinteractions, either at the partonic or hadronic level, motivates the application of concepts of gas or fluid dynamics in their interpretation. Hydrodynamical properties of the expanding matter created in heavy ion reactions have been discussed by Landau [1] (full stopping) and Bjorken [2] (transparency), in theoretical pictures using different initial conditions. In both scenarios, thermal equilibrium is quickly achieved and the subsequent isentropic expansion is governed by hydrodynamics. The relative abundances and kinematic properties of particles provide an important tool for testing whether equilibrium occurs in the course of the collision. In discussing the source characteristics, it is important to measure most of the produced particles in order not to violate conservation laws (e.g. strangeness and charge conservation).

In this letter, we report on the first measurements at RHIC energies of transverse momentum (p_T) spectra of $\pi^{\pm}$ and $K^{\pm}$ over the rapidity range $-0.1 < y < 3.5$ for the 5% most central Au+Au collisions at $\sqrt{s_{NN}} = 200\,\mathrm{GeV}$. The spectra are integrated to obtain yields as a function of rapidity (dN/dy), giving full phase–space (4π) yields. At RHIC energies, a low net–baryon density is observed at mid–rapidity [3], so mesons may be predominantly produced from the decay of the strong color field created initially. At forward rapidities, where primordial baryons are more abundant [4], other production mechanisms, for example associated strangeness production, play a larger role. Therefore, the observed rapidity distributions provide a sensitive test of models describing the space–time evolution of the reaction, such as Landau and Bjorken models [1, 2]. In addition, integrated yields are a key information for statistical models of particle production [5, 6].

BRAHMS consists of two hadron spectrometers, a mid–rapidity arm (MRS) and a forward rapidity arm (FS), as well as a set of detectors for global event characterization [7]. Collision centrality is determined from charged particle multiplicities, measured by scintillator tile and silicon multiplicity arrays located around the nominal interaction point. The interaction vertex is measured with a resolution of 0.6 cm by arrays of Čerenkov counters positioned on either side of the nominal vertex. Particle identification (PID) for momenta below 2 GeV/c is performed via time–of–flight (TOF) in the MRS. In the FS, TOF capabilities allow π–K separation up to $p = 4.5$ GeV/c, and is further extended up to 20 GeV/c using a ring imaging Čerenkov detector. Further details can be found in [7, 8].

Figure 1 presents transverse mass $m_T - m_0$ spectra ($m_T = \sqrt{p_T^2 + m_0^2}$) for π^- and K^-. Particle spectra

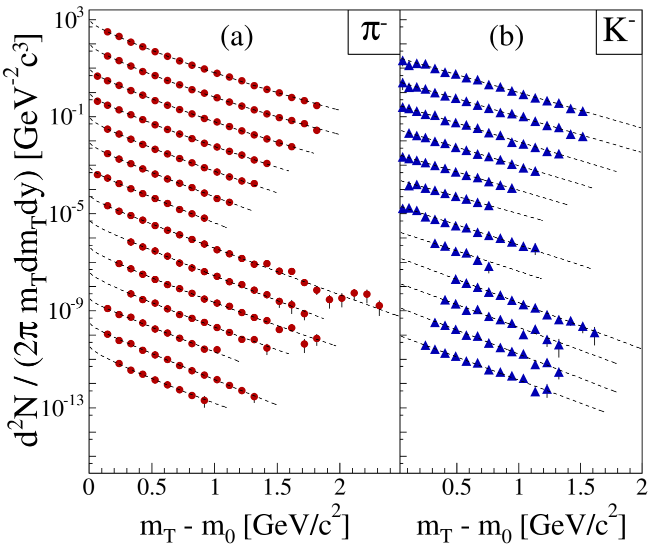

FIG. 1: Invariant transverse mass $m_T - m_0$ spectra of π^- (a) and K^- (b) from $y \sim 0$ (top) to $y \sim 3.5$ (bottom). Dashed lines are fits to the data (see text). Errors are statistical. Spectra have been rescaled by powers of 10 for clarity.

were obtained by combining data from several spectrometer settings (magnetic field and angle), each of which covers a small region of the phase–space (y, p_T). The data have been corrected for the limited acceptance of the spectrometers using a Monte-Carlo calculation simulating the geometry and tracking of the BRAHMS detector system. Detector efficiency, multiple scattering and in–flight decay corrections have been estimated using the same technique. The data have not been corrected for feed–down from resonance and hyperon decays. Details can be found in [8] and references therein.

Fits to the measured spectra are shown as dashed lines in Fig. 1. The pion and kaon spectra are well described at all rapidities by a power law in p_T, $A(1 + p_T/p_0)^{-n}$, and an exponential in $m_T - m_0$, $A \exp\left(\frac{m_T - m_0}{T}\right)$, respectively. The invariant yields dN/dy were calculated by integrating the fit functions over the full p_T or m_T range. The systematic errors on dN/dy, including errors from extrapolation and normalization, amount to $\sim 10\%$ in the range $0 \lesssim y < 1.3$ and $\sim 15\%$ for $y > 1.3$. Preliminary mid–rapidity yields recently reported by the STAR [9] and PHENIX experiments [10] are within $1\,\sigma_{syst}$ of these results. Rapidity densities and mean transverse momenta $\langle p_T \rangle$ extracted from the fits are shown in Fig. 2. Panel (a)

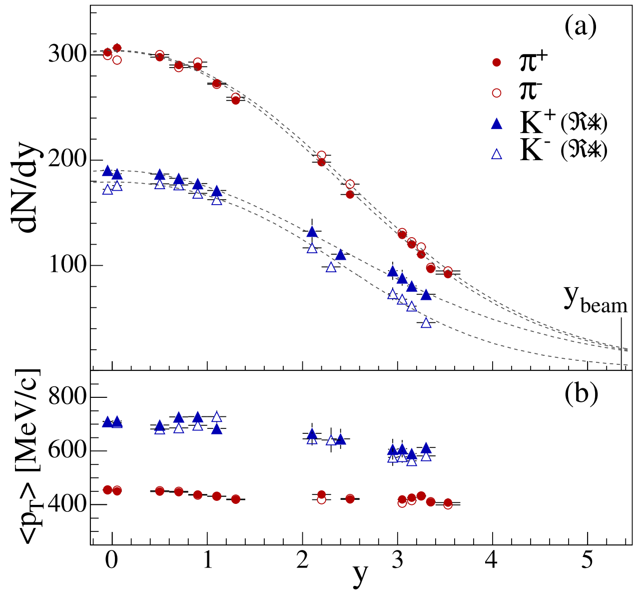

FIG. 2: Pion and kaon rapidity densities as a function of rapidity (a) and mean transverse momentum $\langle p_T \rangle$ (b). Errors are statistical. The kaon yields were multiplied by 4 for clarity. The dashed lines in (a) are Gaussian fits to the dN/dy distributions (see text).

shows the pion and kaon yields. π^+ and π^- are found in nearly equal amounts within the rapidity range covered, while an excess of K^+ over K^- is observed to increase with rapidity [11].

Figure 2(b) shows the rapidity dependence of $\langle p_T \rangle$. There is no significant difference between positive and negative particles of a given mass. For pions, $\langle p_T \rangle = 453 \pm 3$ MeV/c (stat) at $y = 0$ and decreases little to 405 ± 10 MeV/c at $y = 3.5$, while for kaons, $\langle p_T \rangle$ drops from 710 ± 11 MeV/c at $y = 0$ to 590 ± 20 MeV/c at $y = 3.3$ (see [11]).

In order to extract full phase space densities for $\pi^\pm$ and $K^\pm$ we have investigated several fit functions: a single Gaussian centered at $y = 0$ (G1), a sum of two Gaussians (G2) or Woods-Saxon (WS) distributions placed symmetrically around $y = 0$. Our data do not distinguish among these functions, all give a χ^2 per d.o.f. of ~ 1, and have the same total integral to within 2% (cf. Tab. I).

	π^+	π^-	K^+	K^-
WS	1762 ± 17	1777 ± 15	293 ± 6	243 ± 2
G1	1742 ± 15	1767 ± 16	286 ± 5	242 ± 4
G2	1722 ± 17	1738 ± 16	285 ± 5	239 ± 3

TABLE I: Full phase–space yields of $\pi^\pm$ and $K^\pm$ extracted from fits to the dN/dy distributions (see text). Errors are statistical, systematic errors are of the order of 8%.

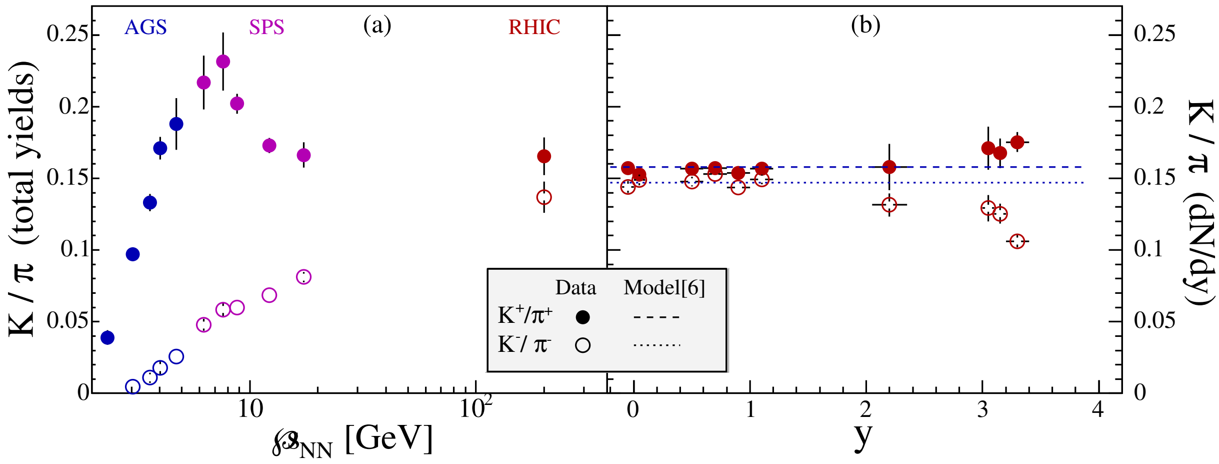

FIG. 3: Full phase–space K/π ratios as a function of $\sqrt{s_{NN}}$ (a) and rapidity systematics at $\sqrt{s_{NN}} = 200\,\mathrm{GeV}$ (b). The dashed and dotted lines in (b) are predictions of the statistical model [6]. Errors are statistical and systematics in (a), only statistical in (b). AGS data are from [12, 13], SPS data from [14–16]. Data points at $\sqrt{s_{NN}} = 6.3\,\mathrm{GeV}$ and $7.6\,\mathrm{GeV}$ [14, 15] are preliminary.

In Fig. 3(a) are shown ratios of the strange to non–strange full phase–space meson yields (K/π) as a function of $\sqrt{s_{NN}}$. The ratio K^+/π^+ shows a fast increase from low AGS to low SPS energies ($\sqrt{s_{NN}} = 8\,\mathrm{GeV}$), followed by a decrease with increasing SPS energy (to $\sqrt{s_{NN}} = 17\,\mathrm{GeV}$). We find, at $\sqrt{s_{NN}} = 200\,\mathrm{GeV}$, a value of $0.165 \pm 0.003 \pm 0.013$, consistent with the ratio at the highest SPS energy. In contrast, K^-/π^- increases monotonically but remains below K^+/π^+. At $\sqrt{s_{NN}} = 200\,\mathrm{GeV}$, it reaches a value of $0.136 \pm 0.002 \pm 0.011$, which is close to K^+/π^+ at the same energy. The full phase–space ratios are not significantly different from those observed in the mid–rapidity region $y \lesssim 1$ (see Fig. 3(b)). Indeed, a fit to a straight line in this particular range gives $K^+/\pi^+ = 0.156 \pm 0.023$ (stat + syst) and $K^-/\pi^- = 0.146 \pm 0.016$. The dashed and dotted lines are predictions of the hadron gas statistical model [6], which used a chemical freeze–out temperature T of 177 MeV and baryo–chemical potential μ_B of 29 MeV (the authors restricted their fits to yields measured in the rapidity range $|y| < 0.5$). The agreement with the data is excellent. However, the data deviate from the model prediction at higher rapidities, where an increasing excess of K^+ over K^- is observed. This is due to an increase of net–baryon densities [3, 4]. A baryon rich environment is favorable for associated strangeness production, e.g. $p + p \rightarrow p + K^+ + \Lambda$, a production channel forbidden to K^-. In the context of the statistical model, this translates into an increase of the baryo–chemical potential μ_B, as already reported in [4], where a calculation by Becattini *et al.* [5] of K^+/K^- vs $\bar{p}/p$ at constant T (and varying μ_B) agrees well with the rapidity dependence of the experimental ratios. It is also known that the chemical freeze–out temperature varies strongly in the AGS energy range but slightly from SPS to RHIC energies (see for example [17]). In this particular energy domain, the K/π systematics are as well mainly driven by changes in μ_B.

The observed pion rapidity distributions exhibit a nearly Gaussian shape. Widths are found to be $\sigma_{\pi^+} = 2.27 \pm 0.02\,(\mathrm{stat})$ and $\sigma_{\pi^-} = 2.31 \pm 0.02$ rapidity units. Similar overall features have already been observed in central Au+Au collisions at AGS [18] and Pb+Pb reactions at SPS [16]. This is reminiscent of the hydrodynamical expansion model proposed by Landau [1]. In the initial state, colliding nuclei are highly Lorentz contracted along the beam direction. Under assumptions of full stopping and isentropic expansion after the initial compression phase (where thermal equilibrium is reached), the hydrodynamical equations, using the equation of state of a relativistic gas of massless particles, lead to dN/dy distributions of Gaussian shape at freeze–out [19]. In a simplified version of the Landau model [20–22] developed for the description of particle production in p+p collisions, the width σ of the pion distribution is formulated as follows:

$$\sigma^2 = \ln \gamma_{beam} = \ln\left(\sqrt{s}/2m_p\right) \tag{1}$$

where m_p is the proton mass. In the context of heavy ion collisions, $\sqrt{s}$ becomes $\sqrt{s_{NN}}$. Figure 4(a) shows $dN/dy(\pi)$ and Landau's Gaussians for $\sqrt{s_{NN}} = 200\,\mathrm{GeV}$ (using Eq. 1 with the condition that the integrals of these Gaussians must be equal to the full–space yields extracted from the data). Surprisingly, a discrepancy of only $\sim 5\%$ between the experimental width and Eq. 1 is observed ($\sigma_{Landau} = 2.16$). However, the analysis of nuclear stopping in central Au+Au collisions at $\sqrt{s_{NN}} = 200\,\mathrm{GeV}$ [3] has demonstrated that about 72% of the participant energy is potentially available for par-

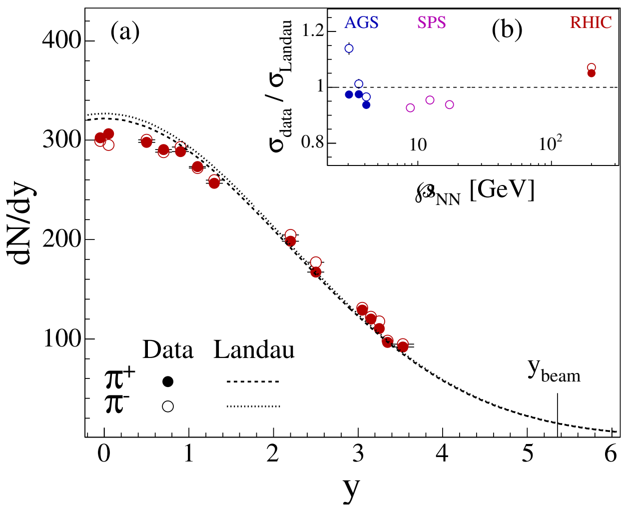

FIG. 4: Comparison $dN/dy(\pi)$ and Landau's prediction at $\sqrt{s_{NN}} = 200\,\text{GeV}$ (a) and ratio $\sigma_{N(\pi)}/\sigma_{Landau}$ as a function of $\sqrt{s_{NN}}$ (b). Errors are statistical.

ticle production, with in fact a large fraction of the energy still carried by particles with large longitudinal momenta. Landau's full stopping assumption therefore does not hold at RHIC. The insert in Fig. 4 shows the ratio $\sigma_{data}/\sigma_{Landau}$ as a function of $\sqrt{s_{NN}}$. At all energies, the widths σ_{data} come from Gaussian fits to the pion distributions. While the difference between theory and measurements is of the order of 10% at most from AGS to RHIC energies, it is worth noting that the overall systematic may not be trivial. The ratio at RHIC is $\sim 15\%$ higher than at SPS.

On the basis of Landau's hydrodynamic, Bjorken [2] proposed a scenario in which yields of produced particles would be boost–invariant within a region around mid–rapidity. In that approach, reactions are described as highly transparent leading to a vanishing net–baryon density around mid-rapidity and particle production from pair creation from the color field in the central zone. This would result in a flat distribution of particle yields around $y = 0$. As mentioned, collisions at RHIC are neither fully stopped nor fully transparent, although a relatively high degree of transparency is observed [3, 4] corresponding to an average rapidity loss of the colliding hadrons of about $\delta y \approx 2$ [3]. Consequently the overall dN/dy distribution of pions is expected to consist of the sum of the particles produced in the boost invariant central zone and the particles produced by the excited fragments. The fact that the observed distributions are flatter at mid-rapidity and wider than those predicted by the Landau–Carruthers model may point in this direction.

In summary, we have measured transverse momentum spectra and inclusive invariant yields of charged meson $\pi^{\pm}$ and $K^{\pm}$. The ratios of strange to non–strange mesons K/π are well reproduced by the hadron gas statistical model [6] that assumes strangeness equilibration at mid–rapidity. The excess of K^+ over K^- yields at higher rapidities is explained by the increasing baryo–chemical potential μ_B with rapidity. The widths of the pion rapidity distributions are in surprising good agreement with Landau–like hydrodynamics, thereby suggesting early thermal equilibration of the source.

This work was supported by the division of Nuclear Physics of the Office of Science of the U.S. DOE, the Danish Natural Science Research Council, the Research Council of Norway, the Polish State Com. for Scientific Research and the Romanian Ministry of Research.

[1] L. D. Landau, Izv. Akad. Nauk SSSR Ser. Fiz. **17**, 51 (1953).
[2] J. D. Bjorken, Phys. Rev. **D27**, 140 (1983).
[3] I. G. Bearden et al. (BRAHMS) (2003), nucl-ex/0312023.
[4] I. G. Bearden et al. (BRAHMS), Phys. Rev. Lett. **90**, 102301 (2003).
[5] F. Becattini, J. Cleymans, A. Keranen, E. Suhonen, and K. Redlich, Phys. Rev. **C64**, 024901 (2001).
[6] P. Braun-Munzinger, D. Magestro, K. Redlich, and J. Stachel, Phys. Lett. **B518**, 41 (2001).
[7] M. Adamczyk et al. (BRAHMS), Nucl. Instrum. Meth. **A499**, 437 (2003).
[8] D. Ouerdane, Ph.D. thesis, University of Copenhagen (2003).
[9] J. Adams et al. (STAR) (2003), nucl-ex/0310004.
[10] S. S. Adler et al. (PHENIX) (2003), nucl-ex/0307022.
[11] BRAHMS, URL `http://www4.rcf.bnl.gov/brahms/WWW/publications.html`.
[12] L. Ahle et al. (E802), Phys. Rev. **C57**, 466 (1998).
[13] L. Ahle et al. (E866 and E917), Phys. Lett. **B476**, 1 (2000).
[14] C. Alt et al. (NA49), J. Phys. **G30**, S119 (2004).
[15] M. Gaździcki et al. (NA49), in *Proceedings of Quark Matter 2004* (2004).
[16] S. V. Afanasiev et al. (NA49), Phys. Rev. **C66**, 054902 (2002).
[17] P. Braun-Munzinger, K. Redlich, and J. Stachel (2003), nucl-th/0304013.
[18] J. L. Klay et al. (E895), Phys. Rev. **C68**, 054905 (2003).
[19] G. A. Milekhin, Zh. Eksp. Teor. Fiz. **35**, 1185 (1958).
[20] P. Carruthers and M. Duong-van, Phys.Lett. **B41**, 597 (1972).
[21] P. Carruthers and M. Duong-van, Phys. Rev. **D8**, 859 (1973).
[22] F. Cooper and E. Schonberg, Phys. Rev. Lett. **30**, 880 (1973).